 doi:10.20944/preprints202010.0104.v1

Surface-Plasmon-Induced Visible Light Photocatalytic Activity of Fe_3O_4/TiO_2 Nanocomposite

Narjes Esmaeili
M. Sc. student, Caspian Faculty of Engineering, College of Engineering, University of Tehran
Rezvanshahr 43861-56387, Iran
narjes.esmaeili@ut.ac.ir

Azadeh Ebrahimian Pirbazari *
Assistant Professor, Fouman Faculty of Engineering, College of Engineering, University of Tehran
Fouman 43516-66456, Iran
*Corresponding author: aebrahimian@ut.ac.ir

Ziba Khodaee
Assistant Professor, University of Applied Science and Technology
Guilan, Iran
zibakhodaee@uast.ac.ir

***Abstract*— In this research, first a binary nanocomposite of magnetic recyclable photocatalyst Fe_3O_4/TiO_2, was synthesized by sol gel technique. Then, in order to enhance the photocatalytic activity of the synthesized nanocomposite, it was deposited by silver nanoparticles for using in degradation of organic pollutants 2, 4-dichlorophenol (2, 4-DCP) under visible light. A range of analytical techniques including XRD, FESEM/EDX, DRS, VSM and N_2 physisorption were employed to reveal the crystal structure, morphology and property of the nanocomposites. We obtained 32% and 55% degradation of 2, 4-DCP under visible light after 180 min irradiation in the presence of Fe_3O_4/TiO_2 and Fe_3O_4/TiO_2/Ag respectively. Thus, the excellent visible light photocatalytic activity of Fe_3O_4/TiO_2/Ag sample can be attributed to the surface plasmon resonance effect of Ag nanoparticles deposited on Fe_3O_4/TiO_2 nanocomposite.**

Keywords- Fe_3O_4; Ag; TiO_2 nanoparticles; Degradation; 2, 4-dichlorophenol;

I. INTRODUCTION

World's population growth and drinking water scarcity has made drinking water supplementation, one of the fundamental problems of today's world. Therefore, water recycling will provide access to a suitable source for various uses. Recently, advanced oxidation processes (AOPs) have been proposed as a wastewater treatment solution. Among advanced oxidation processes, heterogeneous photocatalytic processes have been used as a successful method for the decomposition of various organic pollutants [1]. Photocatalysts are environmental cleaners that can degrade many environmental pollutants through oxidation by using sunlight or artificial light, especially ultraviolet light. Titanium dioxide (TiO_2) is one of the photocatalysts that has been used to degrade organic pollutants. TiO_2 is an ideal photocatalyst with non-toxic nature, high oxidizing properties under UV radiation and low cost, which is stable under various reaction conditions and is also environment friendly [2].
There are two distinct defects in the performance of TiO_2 for the destruction of environmental pollutants. The first is the high energy of its separation band (3.2 eV), which requires UV radiation to generate the electron-cavity pair, but UV radiation forms only about 4% of the sun's emission. In order to utilize a larger part of the radiation emitted from the sun, it is necessary to make special changes in this semiconductor system. Ag, indicating the presence of surface Plasmons resonance (SPR) at the visible light region, which has been used to develop plasmonic photocatalyst [3]. Therefore, the presence of metals such as silver at TiO_2 surface would reduce the separation band energy and expand its absorption spectrum towards the visible light region. The presence of Ag nanoparticles in semiconductors could create Schottky junctions, which decreases recombination rate of electron-cavity pair and also increases the free radicals formation rate [4]. The second defect is the recycling of nano-sized photocatalysts, which is very difficult and costly. An operational solution for photocatalyst

Preprints (www.preprints.org) | NOT PEER-REVIEWED | Posted: 5 October 2020 doi:10.20944/preprints202010.0104.v1

recycling is magnetizing TiO_2 by Fe_3O_4 so that it can be separated and reused by employment of an external magnetic field [5]. This study reports the photocatalytic degradation of 2, 4-DCP under visible light over Fe_3O_4/TiO_2 based photocatalyst containing Ag synthesized via sol-gel method. Physico-chemical characterization of synthesized catalysts has been discussed. The effect of the Ag deposition content on photocatalytic activity has been also investigated.

II. EXPERIMENTAL

A. Materials

$FeCl_3 \cdot 6H_2O$ (Merck No. 103943), $FeSO_4 \cdot 7H_2O$ (Merck No. 103965) were used for synthesis of Fe_3O_4 nanoparticles (NPs). Tetraisopropylorthotitanat (TIP) (Merck No. 8.21895), anhydrous ethanol, ammonia, and High-purity 2, 4-DCP, 98%, (Merck No. 803774) was used as a probe molecule for photocatalytic tests were purchased from Merck Company. Silver nitrate ($AgNO_3$), 99.9%, was supplied by (Merck, No.101510), Acetic acid (CH_3COOH), 99.9% (Merck No. 1.00063). All the reagents were of analytic grade and used without further purification. Double distilled water was used for preparation of all aqueous solutions.

B. Preparation of Fe_3O_4 and TiO_2 NPs

We synthesized Fe_3O_4 nanoparticles by chemical precipitation technique according to Mentioned procedure in ref [6] and for synthesis of TiO_2, the method reported in reference [7] will be used with some modifications. Subsequently, the obtained nanoparticles identified by various analysis.

C. Synthesis of binary (Fe_3O_4/TiO_2) nanocomposite

(Fe_3O_4/TiO_2) nanocomposites Synthesis: We mixed 0.1 g of the Fe_3O_4 nanoparticles with 4 ml of titanium isopropoxide (TIP) (as a titanium source) and 70 ml of water-free ethanol and placed it in an ultrasonic bath for one hour (Solution A). Solution B prepared by mixing 3 ml of acetic acid and 90 ml of distilled water. Then solution B was added to solution A, stirred at 50 °C for 30 min. Finally, after cooling to room temperature, we separate the synthesized solid from the suspension by centrifugation. Rinsed with ethanol and dried for 12 h at 60 °C. For the final step, the obtained solid is heated under atmospheric pressure at 300 °C for one hour.

D. Ag deposited on Fe_3O_4/TiO_2 sample

The prepared Fe_3O_4/TiO_2 sample was deposited by Ag nanoparticles according to reported procedure in ref [7]. 0.5g of Fe_3O_4/TiO_2 was suspended by sonication in 10 mL of deionized water to which $AgNO_3$ (1 mL, 100.0 mM) was added slowly; the resulting solution was stirring at 20°C for 30 min, and then Na_2CO_3 (0.5 mL, 1.0% w/v) was slowly added. The resulting slurry by filtering was separated and dried at room temperature. This nanocomposite was labelled as FTA (a), where (a) is the weight percentage of Ag in the final solid that obtained by EDX analysis.

E. Characterization

The XRD patterns were recorded on a Siemens, D5000 (Germany). The morphology of the prepared samples were characterized using scanning electron microscope (SEM) (Vegall-Tescan Company) equipped with an energy dispersive X-ray (EDX). The diffuse reflectance UV–Vis spectra (DRS) of the samples were recorded by an Ava Spec-2048TEC spectrometer. The nitrogen physisorption measurements were performed with a Quantachrome Autosorb-1-MP (Micromeritics). The BET areas were determined by static nitrogen physisorption at -196 °C subsequent to out-gassing at 200 °C, until the pressure was lower than 5 mbar. All of magnetic measurements have been done by VSM system where is located in the Nano Magnetic Laboratory, in the University of Kashan, Iran, The system is made of Meghnatis Daghighe Kavir, (MDK), Company, Kashan I. R. Iran.

F. Photocatalytic degradation of 2, 4-DCP

In a typical run, the suspension containing 10 mg photocatalyst and 100 mL aqueous solution of 2, 4-DCP (40 mg/L) was stirred first in the dark for 10 min to establish adsorption/desorption equilibrium. Irradiation experiments were carried out in a self-built reactor for 180min irradiation. A visible (Halogen, ECO OSRAM, 500W) lamp was used as irradiation source. At certain intervals, small aliquots (2 mL) were withdrawn and filtered to remove the photocatalyst particles. These aliquots were used for monitoring the degradation progress, with Rayleigh UV-2601 UV/VIS spectrophotometer (λ_{max}= 227nm).

III. RESULT AND DISCUSSION

A. X-ray diffraction analysis

Figure 1. A shows the X-ray diffraction pattern of the synthesized Fe_3O_4 nanoparticles in the present study. The diffractions at 2θ = 30.2°, 35.6°, 43.5°, 54.3° , 57.4° and 63.1° are observed, which are related to the cubic spinel structure of Fe_3O_4, reported by JCPDS reference number 0629-9, thus synthesis of magnetic nanoparticles is confirmed [8].

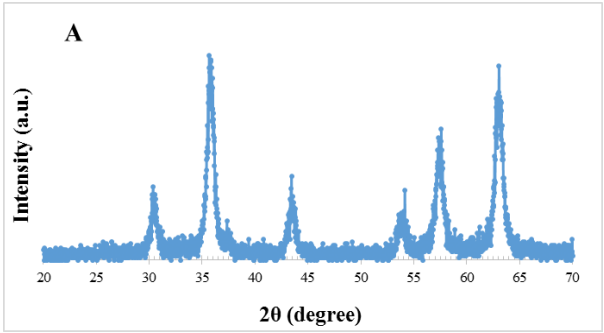

Preprints (www.preprints.org) | NOT PEER-REVIEWED | Posted: 5 October 2020 doi:10.20944/preprints202010.0104.v1

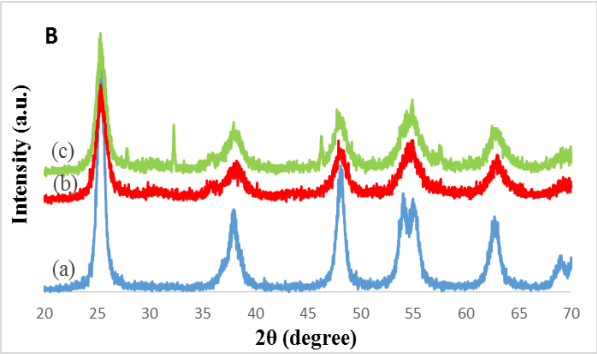

FIGURE 1. XRD patterns of A) Fe_3O_4, B) a) TiO_2, b) Fe_3O_4/TiO_2, and c) $Fe_3O_4/TiO_2/Ag$

Figure 1. B shows the XRD patterns of the pure TiO_2 and Fe_3O_4/TiO_2 and $Fe_3O_4/TiO_2/Ag$ nanocomposites. All the observed diffractions are related to the anatase phase according to the reference (PDF 24-1272) [9]. The reason for the low intensity of Fe_3O_4 nanoparticles and silver atoms diffraction is that they are very small in comparison to TiO_2, and because of the high TiO_2 crystallinity, most of the Fe_3O_4 diffraction is not visible.

The size of the TiO_2 crystal was calculated using first diffraction width and Scherrer's equation. Which varies between 7.11 to 10.38 nm [10].

$$D_{(hkl)} = 0.9\lambda / \beta \cos\theta$$

In this equation, D (hkl) is the crystal size based on Miller's index (101), λ is the wavelength of the X-ray, β is the width of the peak at half of its height, and θ is the Bragg's angle for the desired diffraction. Also, to calculate the parameters (a = b ≠ c), 101 crystalline location of anatase phase is used from the following equation.

$$1/d^2 = \left(h^2 + k^2\right)/a^2 + l^2/c^2$$

In this equation, D, the distance between neighbouring places, is calculated by Bragg's law

$$D_{(hkl)} = \lambda / 2\sin\theta$$

To calculate a = b and c, respectively, the angles of the third (2 0 0) and first (1 0 1) diffractions of the anatase phase are used respectively [11]. Table 1 shows the unit cell parameters and volume for the anatase phase TiO_2 in the synthesized samples and confirmed the formation of pure anatase phase.

TABLE 1. Phase, crystal size and lattice parameters of the prepared samples

Sample	Phase	Crystal size (nm)	a=b (Å)	c (Å)	Cell volume (Å^3)
TiO_2	Anatase	10.38	3.77	9.59	136.30
Fe_3O_4/TiO_2	Anatase	7.11	3.79	9.37	134.87
$Fe_3O_4/TiO_2/Ag$	Anatase	8.31	3.80	9.28	134.40

B. FESEM/EDX analysis

In order to investigate the surface morphology of the synthesized samples, FESEM studies were performed. The FESEM images of pure TiO_2, Fe_3O_4/TiO_2 and $Fe_3O_4/TiO_2/Ag$ samples are shown in Figure 2. The FESEM images of $Fe_3O_4/TiO_2/Ag$ sample show that TiO_2 coated the surface of Fe_3O_4 nanoparticles and Ag nanoparticles deposited on Fe_3O_4/TiO_2 nanocomposite.

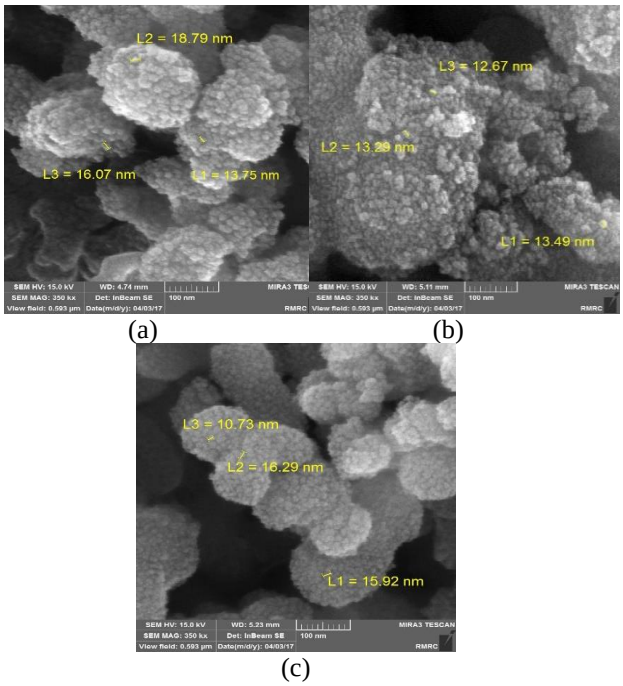

FIGURE 2. FESEM images of a) TiO_2, b) Fe_3O_4/TiO_2, and c) $Fe_3O_4/TiO_2/Ag$

The EDX results were used to examine the elemental composition of the pure TiO_2, Fe_3O_4/TiO_2 and $Fe_3O_4/TiO_2/Ag$ nanocomposites (Figure 3 and Table 2). The EDX result confirms the presence of C, Ti, O, Fe and Ag elements in these samples. In the EDX spectra of $Fe_3O_4/TiO_2/Ag$ sample, the absorption peak at 3 keV is for metallic silver and confirms the presence of silver nanoparticles in the prepared sample. Figure 4 shows elemental mapping images of the prepared samples.

TABLE 2. Elemental chemical analysis of the prepared samples.

Sample	C wt%	O wt%	Ti wt%	Fe wt%	Ag wt%
TiO_2	8.12	41.68	35.96	-	-
Fe_3O_4/TiO_2	6.31	40.15	41.99	1.75	-
$Fe_3O_4/TiO_2/Ag$	8.73	43.84	31.16	1.94	2.09

Preprints (www.preprints.org) | NOT PEER-REVIEWED | Posted: 5 October 2020 doi:10.20944/preprints202010.0104.v1

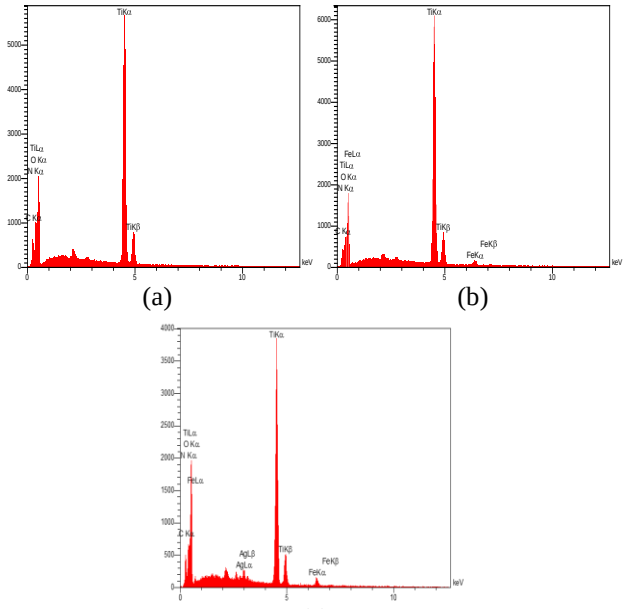

FIGURE 3. EDX spectra of a) TiO_2, b) Fe_3O_4/TiO_2, and c) $Fe_3O_4/TiO_2/Ag$

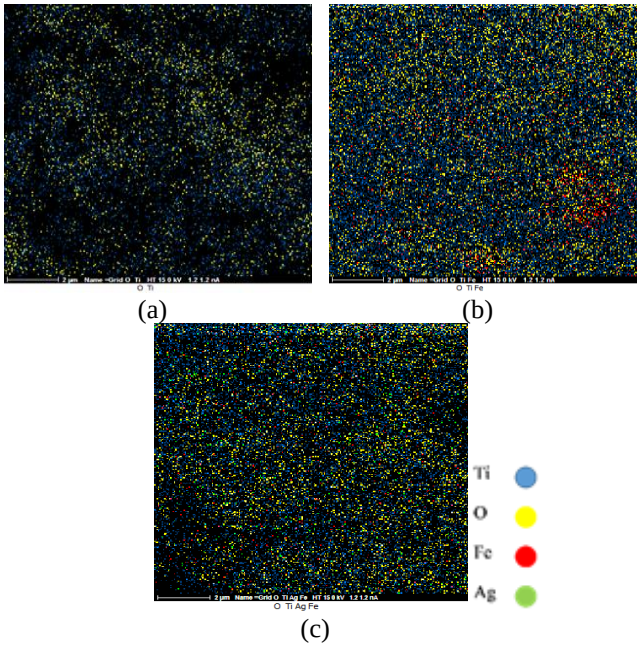

FIGURE 4. Elemental mapping of a) TiO_2, b) Fe_3O_4/TiO_2, and c) $Fe_3O_4/TiO_2/Ag$

C. *DRS analysis*

The diffuse reflectance spectra of the prepared samples over the wavelength range of 200–800 nm are shown in Figure 5. A. The DR spectrum of pure TiO_2 consists of a broad intense absorption around 400 nm, due to the charge-transfer from the valence band formed by 2p orbitals of the oxide anions to the conduction band formed by 3d t_{2g} orbitals of the Ti^{4+} cations [12]. We calculated the band gap energy from the DR spectra according to below equation [13] for the prepared samples.

$$[F(R)h\nu]^{0.5} = A(h\nu - E_g)$$

Where A is constant, F(R) is the Kubelka-Munk function and E_g is the band gap. The band gap of the plasmonic photocatalyst $TiO_2/Fe_3O_4/Ag$ nanocomposite decreased slightly compared with Fe_3O_4/TiO_2 (Table 3).

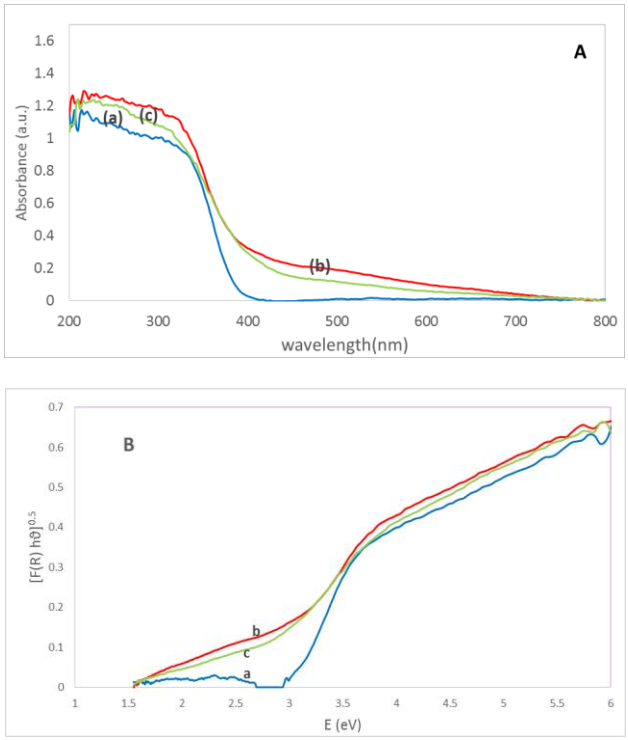

FIGURE 5. A): Diffuse reflectance spectra and B) Kubelka-Munk plots for the band gap energy calculation of a) TiO_2, b) Fe_3O_4/TiO_2, and c) $Fe_3O_4/TiO_2/Ag$

TABLE 3. Band gap energy of the prepared samples.

Sample	TiO_2	Fe_3O_4/TiO_2	$Fe_3O_4/TiO_2/Ag$
E_g (eV)	3.05	2.70	2.60

D. *N_2 physisorption analysis*

N_2 adsorption-desorption isotherms are carried out (Figure 6). The sorption isotherms for all of the prepared samples correspond to the type IV isotherm according to the IUPAC classification [14]. Textural and structural parameters of the obtained samples are shown in Table 4. Specific surface areas and average pore diameter were calculated according to the BET method, pore volumes were derived from the desorption branch according to the BJH model. The BET surface area of ternary nanocomposite ($Fe_3O_4/TiO_2/Ag$ sample) is greater than the starting material (Fe_3O_4/TiO_2 sample), indicating the

Preprints (www.preprints.org) | NOT PEER-REVIEWED | Posted: 5 October 2020 doi:10.20944/preprints202010.0104.v1

deposition of Ag nanoparticles on the surface of Fe_3O_4/TiO_2 nanocomposite.

TABLE 4. Textural and structural parameters of the prepared sample.

Sample	S_{BET} (m^2/g)	Average pore diameter (nm)	Pore volume (cm^3/g)
TiO_2	91.01	7.15	0.17
Fe_3O_4/TiO_2	124.87	4.83	0.25
$Fe_3O_4/TiO_2/Ag$	159.43	5.17	0.19

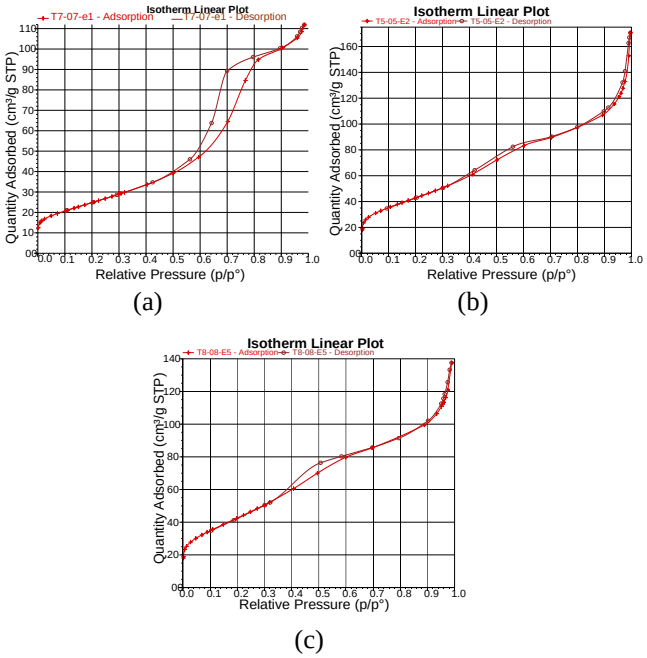

FIGURE 6. N_2 adsorption–desorption isotherms for a) TiO_2, b) Fe_3O_4/TiO_2, and c) $Fe_3O_4/TiO_2/Ag$

E. Magnetic properties of the nanocomposites

In order to evaluate the magnetic response of the magnetic nanocomposites to an external field, the saturation magnetization (Ms) of the samples were measured [15]. The Ms value of the Fe_3O_4 nanoparticles is significantly higher than the Fe_3O_4/TiO_2 and $Fe_3O_4/TiO_2/Ag$ nanocomposites, which is because the Fe_3O_4 nanoparticles are coated with a layer of anatase TiO_2 in the Fe_3O_4/TiO_2 and $Fe_3O_4/TiO_2/Ag$ samples. The small decrease in the Ms value of the $Fe_3O_4/TiO_2/Ag$ sample compared to that of the Fe_3O_4/TiO_2 sample (Figure 7) can be attributed to the slight increase of mass and size due to the adherence of Ag nanoparticles on to the surface of the magnetic composites.

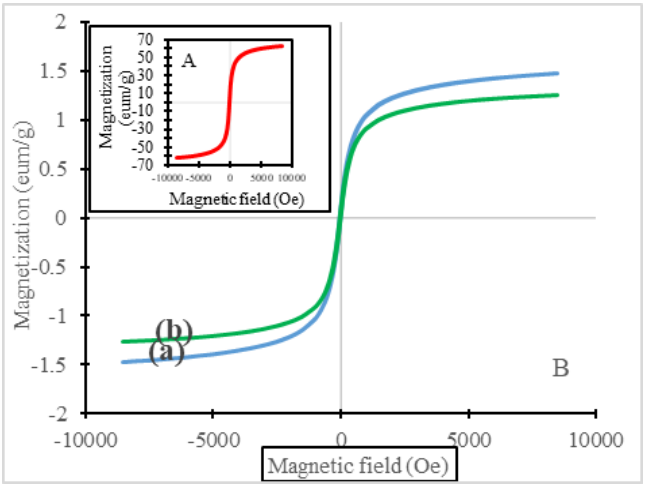

FIGURE 7. Comparison of hysteresis curves of A) Fe_3O_4 and B) (a) Fe_3O_4/TiO_2 and (b) $Fe_3O_4/TiO_2/Ag$

F. Photocatalytic performance of the prepared samples

To evaluate the photocatalytic activity of the synthesized samples a set of experiments for 2, 4-DCP degradation with an initial concentration of 40 mg L^{-1} under visible light at room temperature was carried out in aqueous suspension using TiO_2, Fe_3O_4/TiO_2 and $Fe_3O_4/TiO_2/Ag$ catalysts, and the experimental results are shown in Figure 8. The experimental results demonstrated that among the prepared samples, the $Fe_3O_4/TiO_2/Ag$ catalyst showed the highest efficiency of the 2, 4-DCP degradation under visible light (55% degradation obtained after 180 min irradiation).the results show that the photocatalytic activity of pure TiO_2 is lower than that of Fe_3O_4/TiO_2 and $Fe_3O_4/TiO_2/Ag$ samples. It implies that the Ag promotes the charge pair separation efficiency for TiO_2 catalysts. The electron transfer from the TiO_2 conduction band to Ag particles at the interface is thermodynamically possible because the Fermi level of TiO_2 is higher than that of Ag metal. This results in the formation of a Schottky barrier at metal semiconductor contact region and improves the photocatalytic activity of TiO_2.

Preprints (www.preprints.org) | NOT PEER-REVIEWED | Posted: 5 October 2020 doi:10.20944/preprints202010.0104.v1

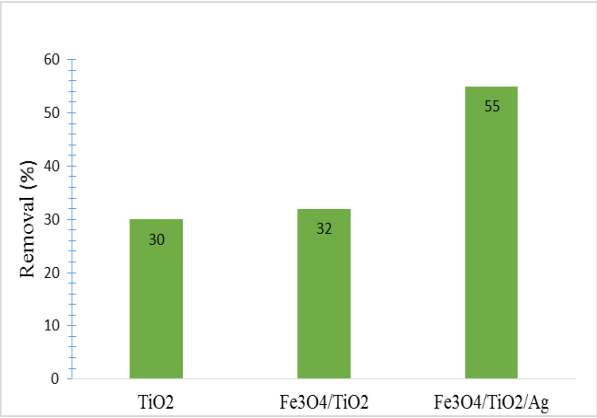

FIGURE 8. Photocatalytic oxidation of 2, 4-DCP in the presence of the prepared samples under visible light (Initial concentration of 2, 4-DCP, 40 mg /L; volume, 100 mL; catalyst dosage, 10 mg, 180 min irradiation).

IV. CONCLUSION

Pure TiO_2 and nanocomposites of Fe_3O_4/TiO_2 and $Fe_3O_4/TiO_2/Ag$ were synthesized by the sol-gel method for degradation of 2, 4-dichlorophenol. The obtained photocatalysts identified by different analysis techniques such as XRD, DRS, N_2 physisorption, VSM and FESEM/EDX. Among all samples, $Fe_3O_4/TiO_2/Ag$ catalyst exhibited the highest photocatalytic activity by 55% degradation under visible light after 180 min irradiation. The high photocatalytic activity can be attributed to both the high the photocatalyst specific surface areas and the plasmon resonance of silver nanoparticles.

ACKNOWLEDGEMENTS

The authors wish to acknowledge the financial support of University of Tehran for supporting of this research.

REFERENCES

[1] R. Ahmad, Z. Ahmad, A.U. Khan, N.R. Mastoi, M. Aslam, J. Kim, Photocatalytic systems as an advanced environmental remediation: Recent developments, limitations and new avenues for applications, Journal of Environmental Chemical Engineering, 4 (2016) 4143-4164.

[2] S. Oros-Ruiz, R. Zanella, B. Prado, Photocatalytic degradation of trimethoprim by metallic nanoparticles supported on TiO_2-P25, Journal of hazardous materials, 263 (2013) 28-35.

[3] W. Hou, S.B. Cronin, A review of surface plasmon resonance-enhanced photocatalysis, Advanced Functional Materials, 23 (2013) 1612-1619.

[4] Y. Tian, T. Tatsuma, Mechanisms and applications of plasmon-induced charge separation at TiO_2 films loaded with gold nanoparticles, Journal of the American Chemical Society, 127 (2005) 7632-7637.

[5] M. Cao, P. Wang, Y. Ao, C. Wang, J. Hou, J. Qian, Photocatalytic degradation of tetrabromobisphenol A by a magnetically separable graphene–TiO_2 composite photocatalyst: mechanism and intermediates analysis, Chemical Engineering Journal, 264 (2015) 113-124.

[6] A.E. Pirbazari, E. Saberikhah, S.H. Kozani, Fe_3O_4–wheat straw: preparation, characterization and its application for methylene blue adsorption, Water Resources and Industry, 7 (2014) 23-37.

[7] C.H. Aguilar, T. Pandiyan, J. Arenas-Alatorre, N. Singh, Oxidation of phenols by TiO_2/Fe_3O_4 M (M= Ag or Au) hybrid composites under visible light, Separation and Purification Technology, 149 (2015) 265-278.

[8] Z. Mo, C. Zhang, R. Guo, S. Meng, J. Zhang, Synthesis of Fe_3O_4 nanoparticles using controlled ammonia vapor diffusion under ultrasonic irradiation, Industrial & Engineering Chemistry Research, 50 (2011) 3534-3539.

[9] A. Stoch, Fly ash from coal combustion-characterization, Energy Engineering and Management, AGH University of Science and Technology, Kraków, Poland, 2015.

[10] M. Khan, W. Cao, Cationic (V, Y)-codoped TiO_2 with enhanced visible light induced photocatalytic activity: A combined experimental and theoretical study, Journal of Applied Physics, 114 (2013) 183514.

[11] A.E. Pirbazari, P. Monazzam, B.F. Kisomi, Cobalt doped TiO_2 : Preparation, characterization and efficient degradation of methyl orange, International Conference on researches in Science and Engineering, Istanbul University, Turkey, 2016.

[12] M. Hamadanian, A. Reisi-Vanani, A. Majedi, Sol-gel preparation and characterization of Co/TiO_2 nanoparticles: application to the degradation of methyl orange, Journal of the Iranian Chemical Society, 7 (2010) S52-S58.

[13] S. Kumar, S. Khanchandani, M. Thirumal, A.K. Ganguli, Achieving enhanced visible-light-driven photocatalysis using type-II $NaNbO_3$/CdS core/shell heterostructures, ACS applied materials & interfaces, 6 (2014) 13221-13233.

[14] K.S. Sing, Reporting physisorption data for gas/solid systems with special reference to the determination of surface area and porosity (Recommendations 1984), Pure and applied chemistry, 57 (1985) 603-619.

[15] Z. Teng, X. Su, G. Chen, C. Tian, H. Li, L. Ai, G. Lu, Superparamagnetic high-magnetization composite microspheres with Fe_3O_4@SiO_2 core and highly crystallized mesoporous TiO_2 shell, Colloids and Surfaces A: Physicochemical and Engineering Aspects, 402 (2012) 60-65.